

Molecular BioSystems

Accepted Manuscript



This is an *Accepted Manuscript*, which has been through the Royal Society of Chemistry peer review process and has been accepted for publication.

Accepted Manuscripts are published online shortly after acceptance, before technical editing, formatting and proof reading. Using this free service, authors can make their results available to the community, in citable form, before we publish the edited article. We will replace this *Accepted Manuscript* with the edited and formatted *Advance Article* as soon as it is available.

You can find more information about *Accepted Manuscripts* in the [Information for Authors](#).

Please note that technical editing may introduce minor changes to the text and/or graphics, which may alter content. The journal's standard [Terms & Conditions](#) and the [Ethical guidelines](#) still apply. In no event shall the Royal Society of Chemistry be held responsible for any errors or omissions in this *Accepted Manuscript* or any consequences arising from the use of any information it contains.



www.rsc.org/molecularbiosystems

Three-dimensional structure and molecular dynamics studies of Prorrenin/renin receptor: description of the active site.

E. Sánchez-Guerrero¹, ME. Hernández-Campos¹, J. Correa-Basurto³, P. López-Sánchez¹, LE. Tolentino-López^{2*}

¹Sección de Estudios de Posgrado e Investigación and ³Laboratorio de Modelado Molecular y Diseño de Fármacos (Laboratory of Molecular Modeling and Drug Design), Escuela Superior de Medicina del IPN, Plan de San Luis y Díaz Mirón, Casco de Santo Tomás, México D.F. 11340, México. ²Laboratorio de Investigación en Química Inorgánica, Escuela Nacional de Ciencias Biológicas del IPN, Prolongación de Carpio y Plan de Ayala s/n, Casco de Santo Tomás, México D.F. 11340, México.

***Corresponding author:** Laboratorio de Investigación en Química Inorgánica, Escuela Nacional de Ciencias Biológicas del IPN, Prolongación de Carpio y Plan de Ayala s/n, Casco de Santo Tomás, México D.F. 11340, México. Tel (+5255) 5729 63 00 ext. 62794, Fax (+5255) 5729 63 00 ext. 62407, E-mail: lugece@hotmail.com

Running Title: Renin/prorenin receptor and peptides modelling.

KEYWORDS: Renin/prorenin receptor, computational modelling, docking, handle peptide, hinge peptide, molecular dynamics.

ABSTRACT. The recent finding of a specific receptor for prorenin/renin (PRR) has brought new insights into the physiology of the renin-angiotensin-aldosterone system. No undoubtable role has been described for this receptor as far. Its role seems to be important in chronic illnesses as hypertension, possibly participating in the cardiovascular remodeling process, and diabetes where participation in inflammation development has been described. It is not possible, however, to explore PRR function using classical pharmacological approaches due to the lack of specific agonists or antagonists. Two synthetic peptides have been described to accomplish these roles, but no conclusive data have been provided. There are no X-ray crystallography studies available to describe structure and potential sites for drug development. So, the aim of this work was to model and theoretically describe the PRR. We describe and characterize the whole receptor protein, its spatial conformation and the potential interactions of PRR with the synthetic peptides available, describing the aminoacids residues responsible of these interactions. This information provides the basis for directed development of drugs, seeking to agonize or antagonize PRR activity and study its function in health and ill stages.

INTRODUCTION

Renin Angiotensin Aldosterone System has increased in complexity with finding of new components. Aside of classical functional roles involving Angiotensin II (Ang II), and its receptors, AT1R and AT2R, the finding of prorenin/renin receptor (PRR) has introduced new insights in its physiology¹. The concept of renin as a ligand with its own receptor it is very interesting. Since its first description, PRR has shown to have a putative role in different hypertension-related pathologies, and although literature is not conclusive in this regard, does not rule out the possibility of its participation on high blood pressure or other illnesses. For instance, PRR has been implicated in inflammation and albuminuria-associated development of nephropathy in streptozotocin-diabetic rats².

The inhibition of PRR action using a peptide derived from the renin prosegment has shown to reduce serum creatinine, left ventricular mass, and cardiac fibrosis and improved cardiac function without affecting blood pressure in spontaneously-hypertensive rats³. Remarkably, Shan et.al. have recently described that PRR may have a role as an indirect system regulator, specifically, modifying the neural control of cardiovascular functions at the supraoptic nucleus in rats, indicating not only the direct action of this receptor upon cardiovascular or renal tissue, but also suggesting that, PRR may participate in superior blood pressure control systems⁴.

Notwithstanding this body of evidence, many of the actions of this receptor remain unclear. It is not possible to generate knockout animals because PRR plays a crucial role in embryonic development⁵. Besides, there is a lack of specific agonists or antagonists helping to characterize it pharmacologically. So far, only two peptides have been described, as an attempt to block or stimulate this receptor. These peptides have been used to mimic the structures of natural ligands. In this regard, they have been named according to the region of the natural peptide from they were taken. So, we have the decoy peptide called "handle" (RILLKKMPVS) region peptide, and the "hinge" (SQGVLKEDVF) peptide⁶. It is not described, however, how they interact or bind to PRR. It is important to describe this interaction of PRR with these and its natural ligands, prorenin and renin, in order to rationally design drugs that block or stimulate this receptor. Moreover, there are several isoforms described as far⁷. The soluble form might interact with drugs proposed on the basis of this work and could have a probable physiological effect not completely understood. Neither it is described the activation or deactivation of PRR when is attached to ATPase6AP2, introducing an exciting field due to its intracellular pH regulation⁸. Also it has been shown that PRR activates Wnt pathways, both canonical and non-canonical, and these paths intervene in cell cycle regulation, hypertrophy and remodelling in several tissues⁹. Once new drugs are available, these fields may be clarified and PRR fully understood.

Computational studies allow solving this question. Several protein-protein interactions have been described using these techniques^{10, 11}. Even more, it is possible to design hypothetical compounds that may interact with the protein of interest and thereafter, they might be synthesized to be evaluated. So, the aim of this work was to develop a computational 3-D model of the PRR in order to study their chemical interactions with the peptides previously mentioned, to understand the molecule-to-molecule interactions and set the basis for a future development of theoretical compounds to inhibit/stimulate PRR.

METHODOLOGY

Primary sequence and amino acid sequence alignment of PRR. The NCBI (GenBank) database (<http://www.ncbi.nlm.nih.gov/genbank/>) was used to search all aminoacids sequences for human PRR. The STRAP alignment program (<http://3d-alignment.e/>) was used to align PRR sequences.

PRR model building and validation. To date, there are no 3D structures available for PRR. This is because 3-D structures for this receptor have not been determined by X-ray crystallography and NMR. Therefore, PRR 3D structure was built based on the genomic sequence data from GenBank [accession number: NP_005756] using Protein Structure Prediction by Pro-Sp3-TASSER server. The PRR model obtained was optimized employing GROMACS program^{12, 13}. The model was analysed with Ramachandran plot and ERRAT server to determine quality of the model^{14, 15}

PRR refinement. The modelled PRR structure was used as macromolecule, for this reason in this work, we decided to refine the PRR 3D model with MD simulations using the GROMACS 4.6.5 software using the OPLS force field^{12, 13}. This methodology has been reported previously in related studies¹⁶. First, we performed a system minimization, using the steepest descent method (50000 steps), to relax steric conflicts generated during setup, followed by all aminoacids residues protonation. All the system was centred in a cubic box and solvated using the simple point charge water model extending up to 10 Å all around the protein¹⁷, and system-neutralized (5 Na⁺ ion by PRR receptor). After energy minimization, the system was submitted to a 100-ps equilibration period restraining the whole protein and the cation positions. Then the whole system was submitted to unrestrained MD simulations lasting 100-ps using NPT and NVT ensembles, maintaining temperature (310° K) and pressure (1 atm) constant. Using the particle mesh Ewald method¹⁸, we calculated electrostatic interactions, with a 1.2-nm cut off for real-space calculation. This cut off was also used for Van der Waals interactions. Temperature, pressure, and number of particles were kept constant for 50 ns MD simulations. Data were analysed using the GROMACS tools package and images and structural representations were prepared using PyMOL v0.99¹⁹. Structural analysis for 3D model was then performed with the VMD v1.9.1 program²⁰, using snapshots every 10 ns from the MD simulations. The trajectory was stored every 10 ps to allow the later retrieval of the root mean square deviation (RMSD) and root mean square fluctuations (RMSF) values using the GROMACS tools program²¹.

Peptides construction and optimization. The peptide-1 (RILLKKMPVS) and peptide-2 (SQGVLEKEDVF) were constructed using the ChemBioDraw v.12.0 software package (<http://www.cambridgesoft.com>), and geometric optimization was initially performed employing the program HYPERCHEM v.7.0 (Hypercube, USA, <http://www.hyper.com>) in the framework of molecular mechanics. The coordinates of peptides minimum geometries were obtained at the B3LYP/6-31G* level of theory using the Gaussian 98 program²².

Identification of binding site residues of PRR. We performed active site analysis using the CASTp server (Computed Atlas of Surface Topography of Protein). This methodology has been previously used in related studies²³, to make the grid required for docking²⁴. The interactions PRR-peptides were examined with Ligplot program (version1.4.5)²¹. This program generates schematic representations of protein-ligand complexes. The PRR-peptide complexes were submitted to this program to identify the binding site residues in the target protein.

Docking Procedure. All different conformations of PRR were taken from the MD simulations every 10 ns, resulting in 10 different snapshots each one, which were taken at specific times of MD such as 10, 20, 30, 40, 50 ns, to study different PRR-peptide interactions that occur in different conformational moments of the receptor molecule. Distinct conformational structures of the PRR were sent to Clus-Pro server (<http://nrc.bu.edu/cluster>) which is a fully automated web-based program for computational docking of protein structures²⁵. Specific protein conformations of the PRR and peptides were uploaded through Clus-Pro web interface. In the docking process, different algorithms evaluate billions of putative complexes, and then it shows a list of most favourable surface complementarities between the protein structures. Moreover, the program output also shows a list of the putative complexes ranked according their clustering properties. Finally, in every case, the most energetically favourable complex was chosen for further studies and to investigate the specific interactions that occur between PRR and the peptides.

RESULTS AND DISCUSSION

Aminoacids sequence and PRR structure prediction

Today, there are few PRR aminoacids sequences reported in the Genbank database, so we decided to perform a multiple alignment of all the sequences submitted and our model. The results obtained showed that only two aminoacids sequences (accession code AAM47531/NP_005756) have been reported. These sequences are fully conserved in human (100%) (Figure 1) We compared these results with the previously reported by Akio E et al.²⁶, who showed that aminoacids sequences are highly homologous in different vertebrates such as rat and mouse (94%), chicken (79%) and fish (68%). Homologous sequences, however, are also found in invertebrates

such as fruit fly (26%), suggesting that PRR is highly conserved at its aminoacids sequence and putative active site is not altered by mutations that may cause structural changes that could affect recognition of prorenin and renin by the receptor. There are reports of mutations within or outside some protein binding sites associated to drug resistance, for instance, ribosomes, β -lactamases and neuraminidase²⁷. Sequence alignment of PRR was performed using Strap alignment program, which showed highly conserved residues between the two sequences as shown in Figure 1. One of the most important parameters to know and describe protein functions is 3D structure,²⁸ providing support for effective experiments design, such as site directed mutagenesis, studies of disease associated mutations or structure-based design of specific ligands.²⁹ The protein structure prediction of PRR was analysed using Pro-SP3-Tasser server³⁰. This program uses a structure prediction algorithm, pro-sp3-Threading/ASSEMBLY/Refinement (TASSER). Structural templates are identified using five different scoring functions included in the threading methods PROSPECTOR-3 and SP3. Top templates identified by each scoring function are combined to derive contact and distance restraints for subsequent model refinement by short TASSER simulations³¹. PRR has four domains: a signal peptide (residues 1-16), an extracellular domain (residues 17-304), a transmembrane domain (residues 305-324) and a cytoplasmic domain (residues 325-350)³², a large unglycosylated amino terminal domain with short cytoplasmic tail¹ (Figure 2a). Our results showed that the secondary structure of PRR exhibited 11 small and large α -helices (V3-V14, G39-M50, N84-L88, L106-E119, N141-E145, L147-R157, E178-E186, Q187-L203, L219-Y226 E231-S253 and A320-Y326) with 3 β -sheets (A74-V80, Y212-E215 and V261-V266); the rest of the sequence consist of loops as shown in Figure 2b. In 3-D structure prediction, refinement required to find structures that are close to native state is a great challenge. Commonly used methods can predict correct topology but such approximate models often lack the resolution required for many important applications, including virtual ligand screening³³. The molecule obtained by modelling was further validated using Ramachandran plot and ERRAT server^{14,15}. Ramachandran plot of phi and psi torsion angles for all aminoacids residues revealed the stereo chemical quality of the 3D structure; showing that 79 % of residues were in favoured regions, 19.9% in allowed regions, and 1.1 % residues in generously outlier region (see supporting information). More than 98 % of the amino acids were in the allowed region and overall quality factor was good. PRR model quality was also validated with the structure-verification server ERRAT, which analyses the statistics of non-bonded interactions between different atoms types; higher scores indicate higher quality¹⁴. The quality obtained by ERRAT server was 92.140 %. None of the residues, however, were above the 99% cut off error value (see supporting information). Given that generally accepted percentage is >50 for *in silico* studies, this confirmed our model reliability.¹⁴

The generated model (putative PRR) is similar to the secondary structure predicted by Akio et al³², where they report 9 α -helices (V3-V14, G39-M50, L106-L116, V149-L158, N177-D206, L219-Y226, S230-Y255 L273-T279 and V305-T324) and 9 β -sheets (E18-K23, S27-F30, A74-K81, V93-L98, V123-L127, V134-M136, L211-L216, A259-V266 and I338-M342). There are several differences, however, related to the number of aminoacids conforming the α -helices and β -sheets; for instance, our model forms 2 α -helices (N84-L88 and V305-T324) not reported by Akio et al.³², and only 3 β -sheets (A74-V80, Y212-E215 and V261-V266). Indeed, our model lacks the other six β -sheets described by Akio et al, (E18-K23, S27-F30, V93-L98, V123-L127, V134-M136 and I338-M342). We think this is because our model was further refined, obtaining different conformations along the molecular dynamics simulation (Figures 1 and 2b). However, to obtain PRR detailed structural information is necessary to carry out long-time MD simulations and the 3-D structure should be determined by experimental work to better understand the changes and the 3-D conformational structures.

MD simulations

Given that crystal and homology models are typically of low resolution, with errors of 3 Å or more in atomic coordinates, we performed MD simulations using GROMACS program to refine and relax the PRR 3D structure obtained³⁴. Our work started analysing stability of PRR 3D structure. Using GROMACS software tools, root mean square deviations (RMSD), and root mean square fluctuation (RMSF) were calculated. The whole system was considered stable at 20 ns in MD simulations. Figure 3 shows the time evolution of the frames RMSD with respect to the initial structure during the last 50 ns of the MD simulations. The RMSD from the starting structure for all backbone C α atoms of the entire protein played an important role in protein stability. Figure 3 represents the PRR RMSD, and shows that protein reaches the convergence to 20 ns with the RMSD value at 0.67 ± 0.07 nm.

The RMSF of PRR C α atoms was plotted to evaluate the average fluctuation of each residue during the simulation. Moreover, RMSF analysis (Figure 4) shows that regions with lowest value start around 0.1 to 0.4 nm, while the regions with high RMSF values oscillated between 0.4 to 0.6 nm, showing high conformational flexibility regions, and corresponding to loop regions on PRR.

Overall structural changes in PRR

Analysing the model of PRR obtained by MD simulations, initial structure exhibited 11 small and large α -helices, 3 β -sheets, with the rest of the sequence consisting of loops. PRR system was stable during simulation and no major secondary structural changes were observed except elongation of two α -helices (N141-E145 and L295-Y297 residues) (Figure 5). These α -helices (N141-E145 and L295-Y297) were shortened and disappeared at different times (20 and 50 ns, respectively), in the MD simulations. However, despite this, entire system was stable throughout the MD simulation, giving reliability to the entire system.

Binding site residues identification and docking of PRR.

Identification and characterization of functional sites on proteins has become an increasingly area of interest. Analysis of active site residues for ligand binding provides insight to enzyme or receptor inhibitors design³⁵. In this study, we report the active site area of PRR as well as the number of aminoacids forming this site. The table 1 and 2 shows the free energy and aminoacids for different active sites of PRR. The predictions of aminoacids participating in the formation of receptor active site shows that these aminoacids are maintained and/or disappear for different conformational moments of PRR, producing several changes in the shape of binding site and consequently altering it, as observed in yellow in Figure 6. In this work, we show that the primary binding site for both peptides is determined mainly by the following amino acid residues (V29, R31, N32, G33, R41, D44, A47, L48, S49, M50, G51, F52, E56, D57, S59, W60, P61, G62, L63, A64, V65, G66, L63, N67, F69, S70, T75, E99, N100, N111, S115, E119, E120, T121, P122, V123, V124, Y252, G257, N258, A259, V260, E262, A264, T265, K267, D270, K287, N288 and Y293) (table 1). These aminoacids are extremely important, because they conform the active site, so it is important to understand and describe their chemical properties, providing the theoretical support to design new molecules to recognize this receptor.³⁶

There are several works about protein-protein interactions³⁷. These kinds of studies allow explaining several biological effects. The binding site residues in our complex (PRR-peptides) were obtained from the Ligand plot program. The results show that a total of 30 aminoacids residues participate in recognition and different modes of binding of peptides 1 and 2 at the binding site of PRR. These aminoacids present different features that allow interactions with peptides residues, i.e., polar or non-polar forming different interactions as π - π interactions, hydrogen bonds and electrostatic attractions with RILLKKMPSV and SQGVLKEDVF (Table 2).

The results of molecular docking show that both peptides may couple to PRR, having affinity (ΔG) and a similar mode of binding, and the amino acids involved in its recognizing are maintained in different conformational stages of the receptor as well (fig 6). It is noteworthy that both peptides also have similar binding mode and binding energies coupled in different 3D structures obtained by MD simulations. Peptide RILLKKMPSV at 0 ns of MD simulation formed different interactions with residues of binding site, being the most important hydrogen bonding interactions: the NH_2 group of R31 with OH of S9, the S of M7 with NH_2 group of R41, the carbonyl oxygen of G51 with the NH_2 group of R1, oxygen carbonyl of L63 with NH_2 group of K5, the OH of T75 with NH_2 K6, carbonyl oxygen of V260 with NH amide of S9 such as NH amide of V260 with carbonyl oxygen of V10, and COO of E262 with OH S9. In the other side, peptide SQGVLKEDVF obtained at 0 ns of simulation, showed that main interactions are formed by hydrogen bonds at the NH_2 group R41 with the carbonyl oxygen of L6, NH amide of V124 interacts with the COO group D9, OH Y252 with amide NH of S2, the carbonyl oxygen of G257 with NH_2 of Q3, NH amide of A259 with the carbonyl oxygen of Q3, NH amide of V264 with the COO group E8, whereas the NH_2 group of K267 interacts with the carbonyl oxygen of F11. Beside the interactions formed by hydrogen bonds as mentioned above, it is important to note the formation of further utility π - π interactions between the aromatic ring of W60 with the aromatic ring in F11.

Throughout different molecular docking moments we could see that these interactions and modes of binding to peptides vary considerably, this is because they form and lose interactions; for example, in the peptide RILLKKMPSV, six electrostatic interactions were formed at time 20, 30 and 50 ns with different amino acids: E262, E119, E120, E56, D57 and S59 with the peptide. In the other hand, peptide SQGVLKEDVF forms only one electrostatic interaction at 30 ns, R41 with D9. Beside these interactions we found three π - π interactions with aromatic aminoacids that form the binding site of PRR, W60, F52 and F11; and a π -cation interaction in R41 and F11. This gain or loss of interactions is reflected in the specific binding energies shown in Table 1.

Conclusion

The data described in the present work are important because they set the basis for development of drugs to stimulate or block PRR. As far, the two peptides in this work are the only ones described that interacts with this receptor: hinge peptide and handle peptide^{6, 38-40}, with non-conclusive actions upon it. In some cases they may act as agonists, but in other, they may interact as antagonists.

We show the hypothetical interactions of PRR and its ligands at molecular level. It is remarkable the interaction with the group of aminoacids described, to conform what it looks like a specific site toward theoretical and experimental efforts might be directed supporting rational design and synthesis of chemical structures which can interact with PRR active site.

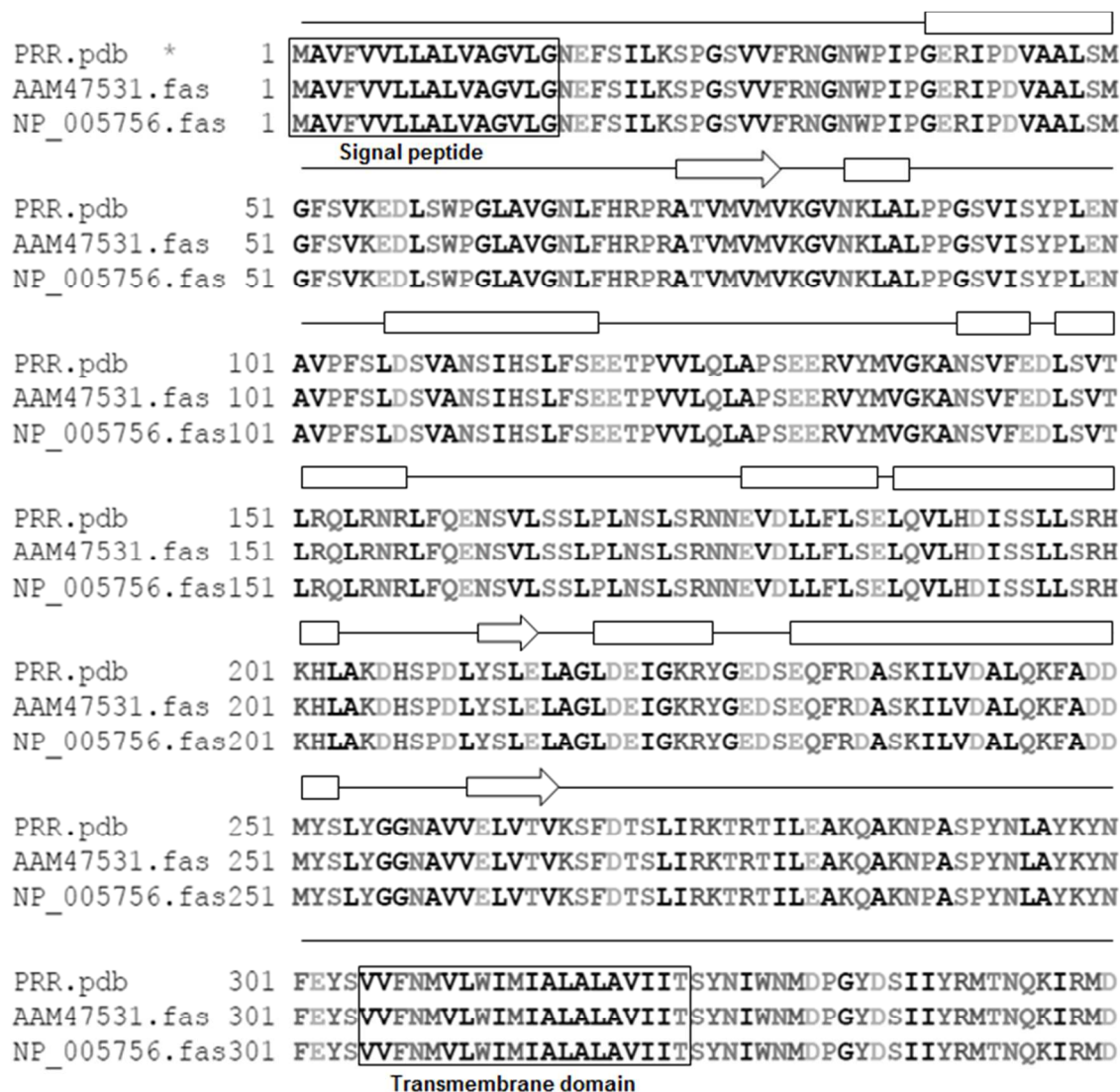


Figure No. 1. Sequences alignment of PRR homologs with STRAP alignment program. The sequences were obtained using Genbank database (accession code AAM47531/NP_005756) and compared to our PRR model. The alignment shows that all amino acid residues are fully conserved and the percentage identity between all sequences of PRR was 100%.

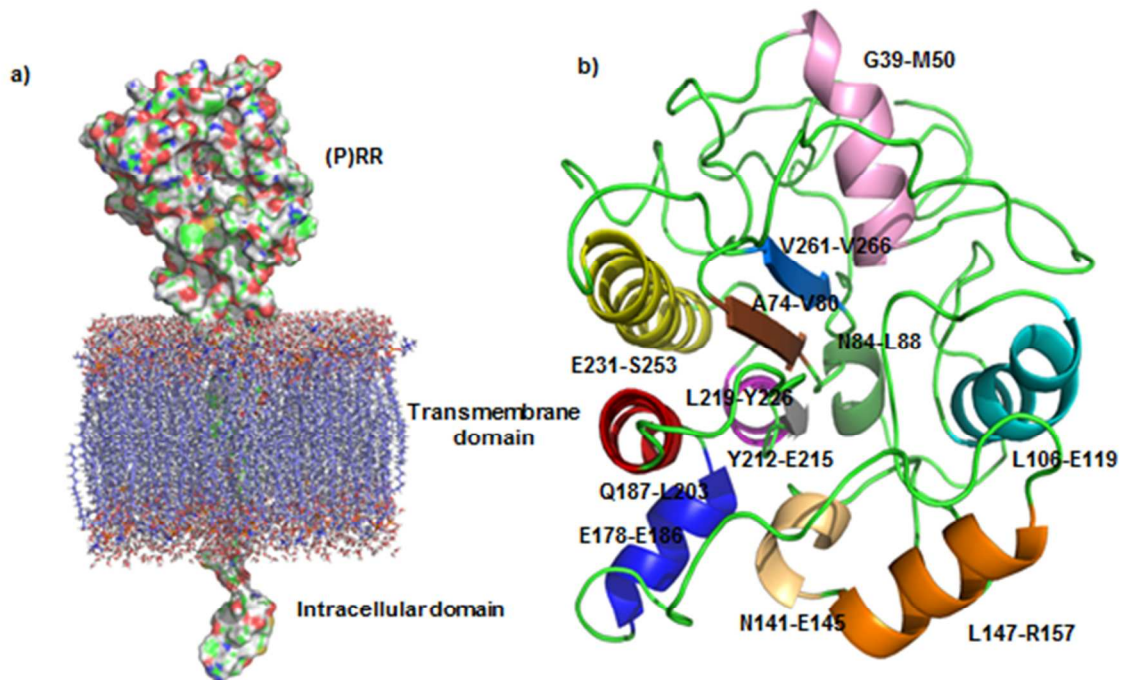


Figure No. 2. a) Structure of PRR formed by intracellular, extracellular domain with transmembrane domain formed with membrane lipids b) secondary structure of PRR with α -helices along (V3-V14, G39-M50, N84-L88, L106-E119, N141-E145, L147-R157, E178-E186, Q187-L203, L219-Y226 E231-S253 and A320-Y326) and β -sheets (A74-V80, Y212-E215 and V261-V266).

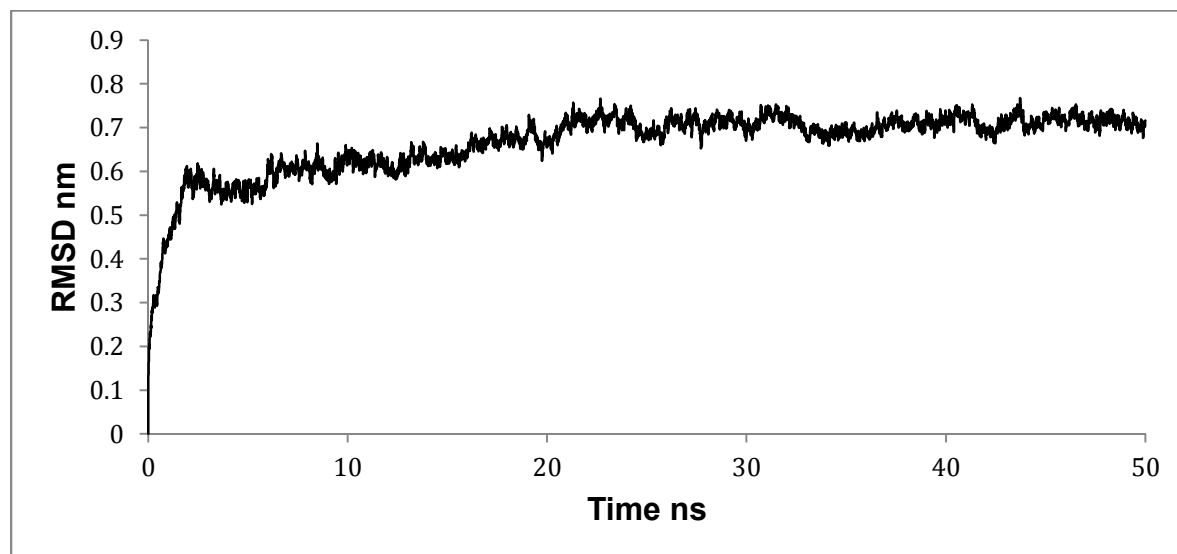


Figure No. 3. Root mean square deviations (RMSD) show that the protein reached structural stability at approximately 20 ns.

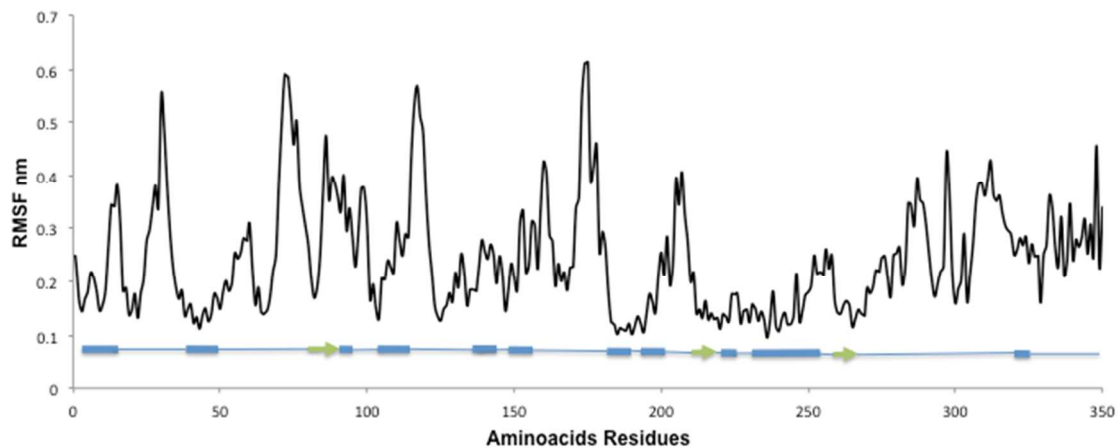


Figure 4. Root mean square fluctuations (RMSF) for PRR model along the simulation period. The coloured line at the bottom indicates fluctuation values in different regions of PRR. Blue blocks correspond to regions where α -helices are located, Thin blue lines correspond to areas where loops are formed, and green arrows indicate areas where β -sheets are formed. Notice that areas corresponding to loops present more apparent fluctuations than α -helices and β -sheets

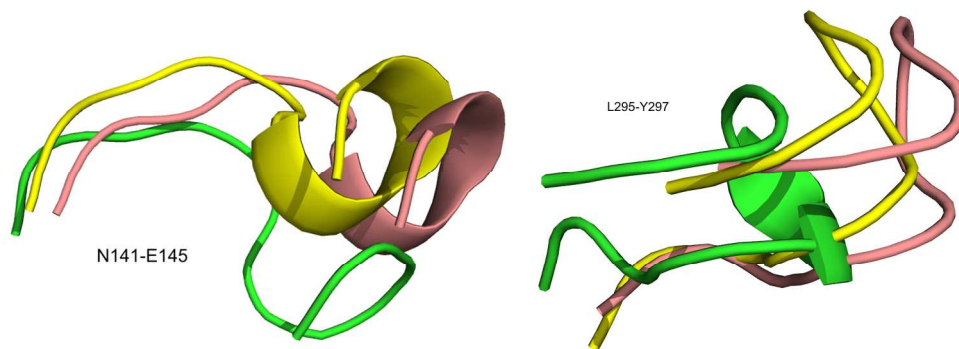


Figure 5. Secondary changes conformational observed in two regions on PRR formed by amino acids residues (N141-E145 and L295-Y297) obtained by MD simulation. Initial 0 ns (green), 20 ns (pink) and 50 ns (yellow) by each time MD simulation.

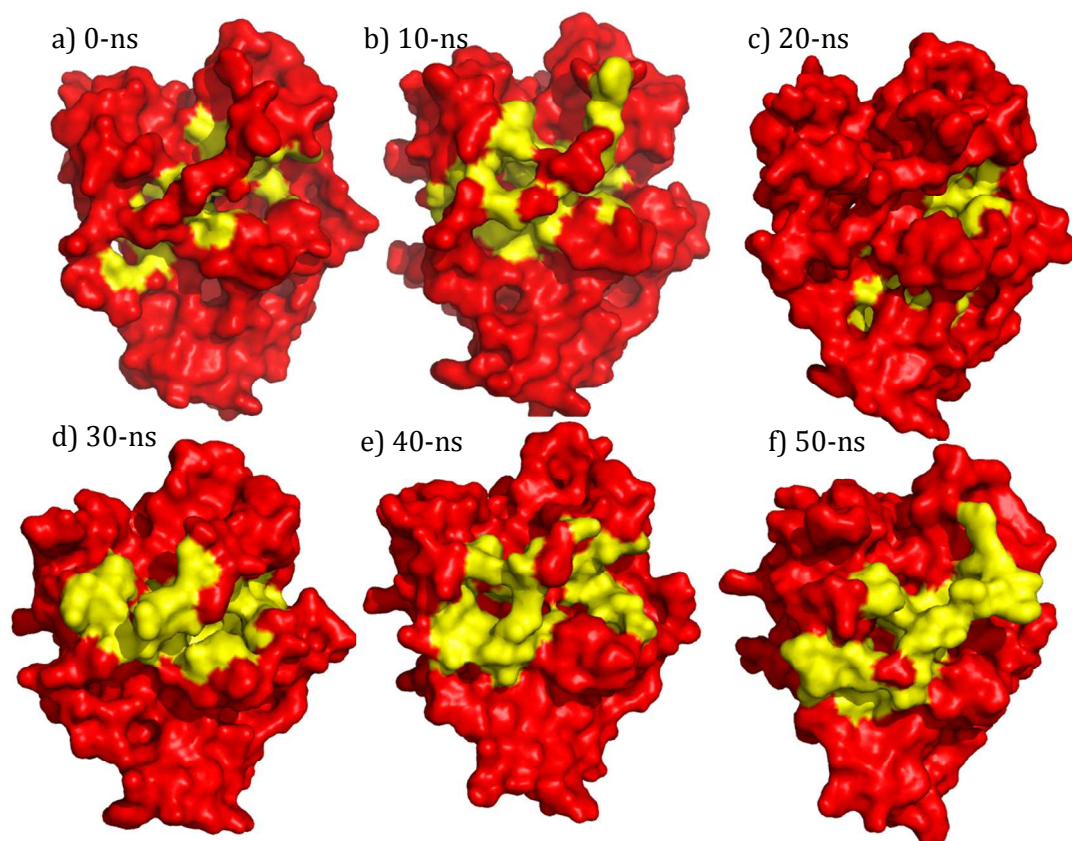


Figure 6. Different forms of the binding site obtained by MD simulation, where the main amino acids residues (yellow) involved in the recognition of peptides with PRR are V29, R31, N32, G33, R41, D44, A47, L48, S49, M50, G51, F52, E56, D57, S59, W60, P61, G62, L63, A64, V65, G66, L63, N67, F69, S70, T75, E99, N100, N111, S115, E119, E120, T121, P122, V123, V124, Y252, G257, N258, A259, V260, E262, A264, T265, K267, D270, K287, N288 and Y293)

Table 1. Aminoacids in PRR active site interacting with synthetic peptides

Peptide	Time (ns)	Energy (Kcal/mol)	Aminoacids participating in peptide binding	Aminoacids participating in peptide binding 3 or more times
RILLKKMPVS	0	-891.9	R31,R41,D44,A47,L48,G51,S53,D57,W60,L63,A64,N67,L68,T75,M79,P103,S108,S112,V123,V124,Q126,L211,Y252,A259,V260,V261,E262,L263,T265	R31, N32, L48, D57,W60, L63, A64, N67, L68, E120, T121, V123, V260, V261, E262, V264
	10	-915.3	R41,L48,S49,M50,D57,L58,W60,P61,L63,N67,L68,P103,D107,S108,N111,L116,E120,T121,P122,V123,V124,V261,E262,L263,V264,T265	
	20	-831.6	V29,R31,N32,G33,M50,F52,V76,V78,V80,L98,E99,N100,L190,L214,L216,A217,E228,F233,L240,L244,F247,A248,V260,E262,V264,V266,S268,F269,D270,T271,S272,K287,A296,Y297	
	30	-859.0	V28,V29,F30,R31,N32,D44,V45,L48,S49,L63,A64,V65,G66,N67,E119,E120,T121,V123,V241,L244,Q245,A248,V260,V261,E262,L263,V264	
	40	-726.9	N32,G33,L48,D57,S59,W60,P61,G62,A64,V65,G66,N67,L68,H70,L116,E120,T121,V123,Y252,A259,V260,V261	
	50	-928.7	A47,L48,G51,F52,S53,E56,D57,S59,W60,P61,L63,A64,V65,G66,N67,L68,F69,H70,R71,P72,P103,E120,T121,V123,V124,V261,L263	
SQGVLKEDVF	0	-869.4	V29,R31,N32,G33,R41,V45,L48,S49,M50,W60,P103,S112,L116,P122,V123,V124,Q126,Y252,G257,N258,A259,E262,L263,V264,T265,K267	V29, R31, N32, G33, R41, V45, A47, L48, M50, F52, W60, P61, G62, L63, A64, N67, L68, S116, T121, P122, V123, V124, N258, A259, V260, V261, E262, I263, V264, T265
	10	-864.8	R31,N32,R41,V45,L48,S59,W60,L63,A64,N67,N111,S112,S115,L116,E119,V123,V260,V261,E262,L263,V264	
	20	-839.5	S27,V28,V29,F30,R31,N32,G33,I37,V45,A46,L48,S49,M50,F52,N67,L68,E228,A248,V260,E262,L263,V264,V266,S268,D270,L273,I274,K287,N288,P289,Y293,Y297	
	30	-755.8	V29,R31,N32,R41,V45,A47,L48,W60,P61,G62,L63,A64,N67,F69,S115,L116,E119,E120,T121,P122,V123,V124,V260,V261,E262,L263,V264	
	40	-761.1	R31,N32,G33,L48,W60,A64,G66,N67,L68,P103,S112,L116,P122,V123,V124,Q126,Y252,259,V260,V261,E262,L263,T265,K267	
	50	-889.5	R41,A47,L48,M50,G51,F52,E56,W60,P61,G62,L63,A64,V65,G66,N67,L68,F69,H70,R71,P72,P103,S108,T121,P122,V123,V124,N258,A259,V261,L263,V264,T265	

Table shows the aminoacids for PRR active site and free energy in different times of MD simulation. Fourth column (from left), shows all aminoacids residues involved in peptide binding through all MD simulation times. Fifth column shows only those aminoacids participating in binding 3 or more times.

Table 2 Interactions between PRR and peptides aminoacids

Interaction (Bonds)	Time (ns)	Peptide (RILLKKMP5V)	PRR	Peptide (SQGLKEDVF)	PRR
Hydrogen	0	S9,M7,R1,K5,K6,S9,V10,S9	R31,R41,G51,L63,T75,V260,V260,E262	L6,D9,S2,Q3,Q3,E8,F11	R41, V124, Y252, G257, A259, V264, K267
	10	K6,K6,K6,R1,V10,K5,K5	L48,S49,M50,N67,N111,T121,V124	F11,Q3,Q3,K7,S2,L6,L6,V10,D9	R31,S59,W60,N67,S115,V123,V124, E262,E262
	20	K5,I2,V10,V10,M7,I2	V29,R31,E99,N100,E262,D270	E8,V5,Q3,Q3,Q3,S2,K4,F11,K7	V29,S49,N67,N67,V260,E262,K287,N288,Y293
	30	S9,S9,V10,K5,R1,K6,P8,M7	R31,D44,V65,V260,E262	F11,S2,Q3,K4,V5,V10,E8	R31, W60, G62, E120, E262, V264
	40	R1,R1,S9,V10,S9,K5,M7,K6,K6	N32,G33,S59,W60,P61,A64,G66,N67,E120	Q3,K7,E8,F11,F11,V5,L6	G33,L48,A64,V123,V124,V260,E262
	50	R1,K5,S9,K5,K5	F52,N67,F69,E120,T121	V10, D9, D9, L6, L6, K4, S2, K7, Q3, Q3, E8	A47,L63,A64,N67,N67,F69,S70,P122,N258,A259,T265
Electrostatic	20	R1	E262	----	----
	30	R1,R1	E119,E120	D9	R41
	50	R1,R1,R1	E56,D57,S59	----	----
π - π	40	----	----	F11	W60
	50	----	----	F11	F52
π -cation	50	----	-----	F11	R41

Table shows interactions between PRR active site aminoacids and both peptides aminoacids in different MD times. Notice that after 20 ns, aminoacids residues change less and stronger bonds appear.

REFERENCES

1. G. Nguyen, F. Delarue, C. Burckle, L. Bouzahir, T. Giller and J. D. Sraer, *J Clin Invest*, 2002, **109**, 1417-1427.
2. P. Balakumar and G. Jagadeesh, *J Cardiovasc Pharmacol*, 2010, **56**, 570-579.
3. T. L. Reudelhuber, *Hypertension*, 2010, **55**, 1071-1074.
4. Z. Shan, P. Shi, A. E. Cuadra, Y. Dong, G. J. Lamont, Q. Li, D. M. Seth, L. G. Navar, M. J. Katovich, C. Sumners and M. K. Raizada, *Circ Res*, 2010, **107**, 934-938.
5. A. Contrepas, J. Walker, A. Koulakoff, K. J. Franek, F. Qadri, C. Giaume, P. Corvol, C. E. Schwartz and G. Nguyen, *Am J Physiol Regul Integr Comp Physiol*, 2009, **297**, R250-257.
6. A. H. Nabi, K. B. Biswas, Y. Arai, T. Nakagawa, A. Ebihara, L. N. Islam and F. Suzuki, *Front Biosci*, 2012, **17**, 389-395.
7. A. H. Jan Danser, W. W. Batenburg and J. H. van Esch, *Nephrol Dial Transplant*, 2007, **22**, 1288-1292.
8. A. Rousselle, G. Sihn, M. Rotteveel and M. Bader, *Clin Sci (Lond)*, 2014, **126**, 529-536.
9. P. Malekar, M. Hagenmueller, A. Anyanwu, S. Buss, M. R. Streit, C. S. Weiss, D. Wolf, J. Riffel, A. Bauer, H. A. Katus and S. E. Hardt, *Hypertension*, 2010, **55**, 939-945.
10. S. Yadav, S. Gupta, C. Selvaraj, P. K. Doharey, A. Verma, S. K. Singh and J. K. Saxena, *PLoS One*, 2014, **9**, e106413.
11. N. Saranya, K. M. Saravanan, M. M. Gromiha and S. Selvaraj, *J Biomol Struct Dyn*, 2015, 1-75.
12. H. J. C. Berendsen, D. van der Spoel and R. van Drunen, *Computer Physics Communications*, 1995, **91**, 43-56.
13. D. Van Der Spoel, E. Lindahl, B. Hess, G. Groenhof, A. E. Mark and H. J. C. Berendsen, *Journal of Computational Chemistry*, 2005, **26**, 1701-1718.
14. G. N. Ramachandran, C. Ramakrishnan and V. Sasisekharan, *J Mol Biol*, 1963, **7**, 95-99.
15. C. Colovos and T. O. Yeates, *Protein Sci*, 1993, **2**, 1511-1519.
16. M. Bello and J. Correa-Basurto, *PLoS One*, 2013, **8**, e72575.
17. B. Pullman, ed., *Intermolecular Forces*, Springer, Jerusalem, 1981.
18. T. Darden, D. York and L. Pedersen, *The Journal of Chemical Physics*, 1993, **98**, 10089-10092.
19. M. Lill and M. Danielson, *Journal of Computer-Aided Molecular Design*, 2011, **25**, 13-19.
20. W. Humphrey, A. Dalke and K. Schulten, *Journal of Molecular Graphics*, 1996, **14**, 33-38.
21. M. Lundborg and E. Lindahl, *The Journal of Physical Chemistry B*, 2014, **119**, 810-823.
22. G. W. T. M. J. Frisch, H. B. Schlegel, G. E. Scuseria, M. A. Robb, J. R. Cheeseman, V. G. Zakrzewski, J. A. Montgomery, R. E. Stratmann, J. C. Burant, S. Dapprich, J. M. Millam, A. D. Daniels, K. N. Kudin, M. C. Strain, O. Farkas, J. Tomasi, V. Barone, M. Cossi, R. Cammi, B. Mennucci, C. Pomelli, C. Adamo, S. Clifford, J. Ochterski, G. A. Petersson, P. Y. Ayala, Q. Cui, K. Morokuma, D. K. Malick, A. D. Rabuck, K.

- Raghavachari, J. B. Foresman, J. Cioslowski, J. V. Ortiz, B. B. Stefanov, G. Liu, A. Liashenko, P. Piskorz, I. Komaromi, R. Gomperts, R. L. Martin, D. J. Fox, , T. Keith, M. A. Al-Laham, C. Y. Peng, A. Nanayakkara, C. Gonzalez, M. Challacombe, P. M. W. Gill, B. G. Johnson, W. Chen, M. W. Wong, J. L. Andres, M. Head-Gordon, E. S. Replogle, and J. A. Pople, *Gaussian 98 (Revision A.9)*, 1998.
23. M. A. Hasan, S. M. Alauddin, M. Al Amin, S. M. Nur and A. Mannan, *Drug Target Insights*, 2014, **8**, 1-9.
 24. J. Dundas, Z. Ouyang, J. Tseng, A. Binkowski, Y. Turpaz and J. Liang, *Nucleic Acids Res*, 2006, **34**, W116-118.
 25. S. R. Comeau, D. W. Gatchell, S. Vajda and C. J. Camacho, *Bioinformatics*, 2004, **20**, 45-50.
 26. A. H. Nabi, K. B. Biswas, Y. Arai, T. Nakagawa, A. Ebihara, L. N. Islam and F. Suzuki, *Front Biosci (Landmark Ed)*, **17**, 389-395.
 27. L. Tolentino-Lopez, A. Segura-Cabrera, P. Reyes-Loyola, M. Zimic, M. Quiliano, V. Briz, A. Munoz-Fernandez, M. Rodriguez-Perez, I. Ilizaliturri-Flores and J. Correa-Basurto, *Biopolymers*, 2012, **99**, 10-21.
 28. L. A. Kelley and M. J. Sternberg, *Nat Protoc*, 2009, **4**, 363-371.
 29. L. I. Fidanova S, *Analele Universitatii de Vest, Timisoara*, 2009, **XLVII**, 33-46.
 30. H. Zhou and J. Skolnick, *Biophysical Journal*, **96**, 2119-2127.
 31. H. Zhou, S. B. Pandit and J. Skolnick, *Proteins*, 2009, **77 Suppl 9**, 123-127.
 32. A. Ebihara, T. Nakagawa, C. Nakane, N. A. Nabi and F. Suzuki, *Front Biosci (Elite Ed)*, 2012, **4**, 1150-1156.
 33. A. Jagielska, L. Wroblewska and J. Skolnick, *Proc Natl Acad Sci U S A*, 2008, **105**, 8268-8273.
 34. S. Osuna, G. Jimenez-Oses, E. L. Noey and K. N. Houk, *Acc Chem Res*, 2015.
 35. X. Zhao, Q. Ning, M. Ai, H. Chai and M. Yin, *Mol Biosyst*, 2015, **11**, 923-929.
 36. A. Elengoe, M. Naser and S. Hamdan, *International Journal of Molecular Sciences*, 2014, **15**, 6797-6814.
 37. J. D. Alsop and J. C. Mitchell, *Proteins*, 2015.
 38. M. He, L. Zhang, Y. Shao, X. Wang, Y. Huang, T. Yao and L. Lu, *Eur J Pharmacol*, 2009, **606**, 155-161.
 39. A. Ichihara, M. Hayashi, Y. Kaneshiro, F. Suzuki, T. Nakagawa, Y. Tada, Y. Koura, A. Nishiyama, H. Okada, M. N. Uddin, A. H. Nabi, Y. Ishida, T. Inagami and T. Saruta, *J Clin Invest*, 2004, **114**, 1128-1135.
 40. A. Ichihara, F. Suzuki, T. Nakagawa, Y. Kaneshiro, T. Takemitsu, M. Sakoda, A. H. Nabi, A. Nishiyama, T. Sugaya, M. Hayashi and T. Inagami, *J Am Soc Nephrol*, 2006, **17**, 1950-1961.

Acknowledgments. This work was supported by SIP20140636 and SIP20150467 grants.